Title: Plasticity of gene expression in the nervous system by exposure to environmental odorants that inhibit HDACs

The author list: Sachiko Haga-Yamanaka[*,1], Rogelio Nunez-Flores[*,1,5], Christi Ann Scott[*,2], Sarah Perry[3], Stephanie Turner Chen[2], Crystal Pontrello[1], Meera Goh Nair[5] and Anandasankar Ray[1,2,3]

ADDRESS:

[1]Department of Molecular, Cell and Systems Biology

[2]Cell, Molecular and Developmental Biology Program

[3]Genetics, Genomics and Bioinformatics Program

[4]Department of Nematology

[5]Division of Biomedical Sciences

University of California, Riverside, CA 92521, USA

* these authors contributed equally

CORRESPONDING AUTHOR: Anandasankar Ray

Department of Molecular Cell and Systems Biology, University of California Riverside, 3401 Watkins Drive, Riverside, CA 92521, USA

CONTACT INFORMATION : Phone: +1(951) 827-5998, Email: anand.ray@ucr.edu

ABSTRACT

Eukaryotes are often exposed to microbes and respond to their secreted metabolites, such as the microbiome in animals or commensal bacteria in roots. Little is known about the effects of long-term exposure to volatile chemicals emitted by microbes, or other volatiles that we are exposed to over a long duration. Using the model system *Drosophila melanogaster* we evaluate a yeast emitted volatile, diacetyl, found in high levels around fermenting fruits where they spend long periods of time. We find that exposure to just the headspace containing the volatile molecules can alter gene expression in the antenna. Experiments showed that diacetyl and structurally related volatile compounds inhibited human histone-deacetylases (HDACs), increased histone-H3K9 acetylation in human cells, and caused wide changes in gene expression in both *Drosophila* and mice. Diacetyl crosses the blood-brain barrier and exposure causes modulation of gene expression in the brain, therefore has potential as a therapeutic. Using two separate disease models known to be responsive to HDAC-inhibitors, we evaluated physiological effects of volatile exposure. First, we find that the HDAC inhibitor also halts proliferation of a neuroblastoma cell line in culture as predicted. Next, exposure to vapors slows progression of neurodegeneration in a *Drosophila* model for Huntington's disease. These changes strongly suggest that unbeknown to us, certain volatiles in the surroundings can have profound effects on histone acetylation, gene expression and physiology in animals.

SIGNIFICANCE STATEMENT

Volatile compounds are ubiquitous and are produced by most organisms. We report that some volatile compounds emitted from microbes and present in food, can alter epigenetic states in neurons and other eukaryotic cells. These volatile organic compounds act as inhibitors of HDACs and over time periods of hours and days cause dramatic modulation of gene expression even from

a physically separated emission source. Given their HDAC-inhibitory properties the VOCs also act as therapeutics in preventing proliferation of neuroblastoma cells and degeneration of neurons in a Huntington's disease model.

TEXT

Multicellular organisms evolve in the presence of microbial volatiles and metabolites (1, 2), often for prolonged periods of time. Human-associated microbes have incredible metabolic diversity, encoding 100x as many genes as the human genome itself and most of the genetic differences that distinguish any two people (1). It is estimated that about half of the thousands of metabolites found in mammalian blood are either produced or altered by microbes (3). Microbial metabolites are an important mechanism by which the microbiome influences host immunity amongst other things (2, 4). Many volatiles are also generated from the metabolism of a variety of food components, including triglycerides, sugars and amino acids (5). Some chemicals are also produced by microorganisms such as yeasts and lactic bacteria during fermentation in many foods and beverages (5).

Previous studies using CO_2 have demonstrated that prolonged exposure of ~5 days can cause increase in volume of the CO_2-sensitive V-glomerulus in the antennal lobe, which can lead to adaptations in fly behavior (6, 7)(7, 8). In order to study the physiological effects of long-term exposure to microbial volatiles, we exposed flies for 5 days to diacetyl, a buttery odorant made by yeast in fermenting fruits at high levels (1350 ppb in ripe banana), and is also found in many commonly consumed foods such as butter, yoghurt, wine, fruits, beer, popcorn (5, 9-11). Diacetyl was selected for two reasons: first, *Drosophila melanogaster* use fermenting fruits as their favored

food source, oviposition site and spend long durations of time exposed to it. Second, diacetyl is known to be an inhibitory odorant of the CO_2 receptor and therefore an opposite effect is expected on the V-glomerulus from the previous study (12). Follow up experiments revealed that diacetyl acts as an HDAC inhibitor in vitro. We found that volatiles structurally similar to diacetyl have similar HDAC-inhibitory properties as well. Subsequent analyses with two different model systems: *Drosophila melanogaster* and *Mus musculus* showed gene expression changes in tissues caused by odor exposure from a distant source. We found expression of hundreds of genes to be modulated upon exposure to the volatile, as would be expected from an inhibitor of HDACs. HDACs are histone-modifying enzymes involved in the removal of acetyl groups from lysine residues and the remodeling of chromatin structure as a means to regulate gene expression (13, 14). With large-scale roles in gene regulation, HDACs are promising targets in drug development for many diseases such as cancers and neurodegenerative disorders (15-17). Several classes of orally administered HDAC inhibitors have been found to attenuate the progression of certain cancers and neurodegenerative diseases including Alzheimer's disease and Huntington's disease (17). We find that exposure to diacetyl volatiles can substantially alter gene expression in the mouse brain, presumably by crossing the blood-brain barrier. The exposure slows degeneration of photoreceptor cells in a Huntington's disease model in *Drosophila*. Additionally, exposure to diacetyl shows dramatic reduction in proliferation of a neuroblastoma cell line in culture. Our discovery of a family of volatile odorants that also act as HDAC inhibitors highlights a need to understand how small molecules present in our environment interact with and alter eukaryotic gene expression.

RESULTS

Activity-dependent expression modulation of chemosensory receptors

To assess the effect of CO_2 response inhibitor diacetyl on the antennal lobe, flies were exposed to the odorant during the first days immediately following eclosion. *Gr63a-Gal4* and *Gr21a-Gal4* flies were exposed to diacetyl at 10^{-2} from two to five days in an air-tight container, and then imaged for expression of GFP in the CO_2 receptor expressing ab1C neurons of the antenna, as well as the V glom erulus, which receives axonal input from ab1C neurons (18). Surprisingly, *Gr63a* promoter driven GFP signal in the V glomerulus is completely abolished after 5 days of exposure to the odor for all brains collected (Figure 1A,1B). However, there is a concomitant decrease in GFP+ ab1C neurons in the antenna (Figure 1A). Similar results were seen for *Gr21a* driven expression, where expression of GFP was lost in both the V-glomerulus and ab1C neurons (Figure S1A, S1B). However, after five days of recovery in clean air GFP expression is regained in the V-glomerulus as well as in ab1C neurons, indicating that both *Gr21a* and *Gr63a* expression has been restored (Figure S2). Because olfactory neurons do not regenerate in the fruit fly (19, 20), we can conclude that this gain in expression is most likely due to a change in gene regulation and not due to neuronal cell death.

In order to test whether expression of *Gr63a* and *Gr21a* is being down regulated by diacetyl we relied on quantitative-PCR along with a few members of the *Or* family. The receptor genes tested include ones that are in neurons that diacetyl inhibits (Gr21and Gr63a), no activity (Or47a, Or88a) or a broadly expressed co-receptor (Or83b). Wild-type flies that were exposed to diacetyl for 6 days showed dramatic down regulation in all genes tested. However, after a 5-day recovery period expression of all the genes except *Or88a* recovered, including *Gr63a* (Fig S1C). This form of plasticity in gene expression is unexpected and the mechanism important to find.

Diacetyl and structurally related odorants act as HDAC inhibitors vitro

Diacetyl is structurally related to a soluble metabolite secreted by the gut microbiome and liver, β-hydroxybutyrate, which is known to target zinc-dependent HDACs(21) (Figure 1A). It is also related to another known HDAC inhibitor Sodium butyrate. Diacetyl is present widely in nature as a pH-neutral fermentation product of microorganisms such as yeasts in over-ripe fruit, the favorite food for *Drosophila*, and also from lactic acid bacteria, and is found in many foods and beverages (5) (Table S1). In humans, diacetyl is also produced by microbes on the skin, in the oral cavity, and is found in breath (22). Interestingly, this volatile is known to traverse the cell membrane (23). Soluble metabolites from the gut microbiome, like short chain fatty acids, are known to affect histone modifying enzymes,(1, 24), gene expression, and physiology in various parts of the host. It is presumed that these dissolved compounds absorbed in the blood circulate to various parts of the body. Additionally, microbes in our skin microbiome, mouth microbiome, and environment also emit a diverse repertoire of volatile metabolites that can traverse much greater distances away from the source. For example, characteristic body odor is caused mainly by the skin microbiome (25). To examine if diacetyl can directly modulate HDACs like β-hydroxybutyrate, we performed in vitro acetylation assays with recombinant human HDACs. We found that indeed, diacetyl inhibited all 4 purified human Class I HDACs (HDAC1, 2, 3 and 8) and 1 Class II HDAC (HDAC6). The inhibition occurred in a dose-dependent manner in the in vitro assay, albeit to different extents. The IC_{50} values for HDAC1, 2, 3, 8 and 6 were 7.3 mM, 23.1 mM, 7.5 mM, 14.3 mM and 24.5 mM respectively (Figure 1B). The levels of inhibition as observed from IC50 values for HDAC1 and HDAC3 are comparable to those of β-hydroxybutyrate (21).

To test other odorants for their ability to inhibit HDACs, we identified a list of volatile odorants structurally similar to diacetyl using the similarity search feature on Pubchem and cross-

142 referenced them with known odorants and tested them on four purified human HDACs, from Class
143 I (HDAC1 and HDAC3) and Class II (HDAC4 and HDAC6). Each compound was tested at 15
144 mM, the concentration at which diacetyl inhibits HDAC1, 3, and 6 with more than 50% efficacy
145 (Figure 1C, D). All compounds tested reduced the activity of at least one of the HDACs (Figure
146 1D). Ethyl pyruvate, methyl pyruvate, 2,3-hexanedione, 2,3-heptandione, 2,3-pentandione
147 inhibited HDAC1, 3 and 6 with more than 70% efficacy. Allyl butyrate also similarly inhibited
148 those HDACs but with lower efficacy. 1-acetoxyacetone, and 2,3-butanediol inhibited HDAC6
149 more than 70% but inhibitory effects against HDAC1 and 4 were lower. Moreover, propyl formate
150 strongly inhibited HDAC 6 but did not inhibit HDAC1, 3, and 4. Taken together, these results
151 indicate that microbial volatiles and structurally related odorants have the ability to inhibit human
152 HDACs, and that each compound has specific HDAC inhibitory properties.

153 **Microbial volatile increases histone acetylation in human cell nuclei**

154 In order to directly examine histone acetylation at the cellular level, we used human
155 HEK293 cells which offer a tractable system to prepare nuclear extracts and picked one volatile to
156 test in more detail. We exposed the cells to different doses of diacetyl for 2 or 6 hours and
157 monitored histone acetylation levels within nuclear extracts in Western Blot assays. Compared to
158 the mock treatment, 10 mM diacetyl significantly increased H3K9 acetylation levels within 2 hours
159 of treatment, whereas the acetylation levels of H3K14 and H4K5 were not affected (Figure 2A).
160 This specificity for an increase of the H3K9 mark is consistent with previous observations for β-
161 hydroxybutyrate (21). After 6 hours of treatment, the H3K9 acetylation induced by 10 mM diacetyl
162 was further increased (Figure 2B). The increase in H3K9 acetylation with diacetyl treatment is
163 dependent both on the duration of exposure and concentration of the odorant.

Organisms are constantly exposed to volatiles commonly found in their food and environment for prolonged periods of time. In order to test the effect of a lower concentration of the volatiles, we selected a 5-day exposure time at a 100-fold lower concentration. When we treated HEK293 cells with this lower dose of diacetyl (100 μM), H3K9 acetylation level increased after 96 hours of exposure and reached significantly higher levels than control after 120 hours (Figure 2C,D). These results demonstrate that even prolonged exposure to low levels of diacetyl can greatly impact the epigenetic landscape inside the nucleus. More importantly, a 5-day exposure was sufficient to alter the epigenetic state of nuclei at concentrations that are present in some food sources. Taken together, these results demonstrate that diacetyl can act as an HDAC inhibitor, with the potential of causing broad modulations of gene expression, histone acetylation in cells, and inhibition of purified HDAC enzymes in a dose-dependent manner.

Transcriptional response to odor exposure is conserved in invertebrates and vertebrates

We next performed in vivo experiments to determine whether eukaryotic cells alter gene expression in response to diacetyl exposure, as would be expected with HDAC-inhibition. Epigenetic changes occur slowly over days, and to test its effects on gene expression we used two model systems for eukaryotes: invertebrates (*Drosophila melanogaster)* and vertebrates *(Mus musculus).* We placed *Drosophila* adult males in vials and housed these vials within a closed container exposed to headspace from a 1% diacetyl solution (in paraffin oil) for 5 days, as in a previous long-term odor-exposure study (7) (Figure 3A). The transcriptome of the primary olfactory organ, the antenna, was compared with that of the control group of age-matched flies that were exposed to the solvent paraffin oil (PO). The antennal transcriptional profile of diacetyl-exposed flies showed substantial changes in gene expression when compared to the solvent control (Figure 3B). We identified 1234 differentially-expressed genes (DEGs) (false discovery rate, FDR

187 < 0.05) in the antennal transcriptome of diacetyl-exposed flies compared to control animals. Of
188 these, 645 genes were significantly up-regulated ($\log_2$ fold-change > 1; red dots in Figure 3B) and
189 589 genes were significantly down-regulated ($\log_2$ fold-change < -1; blue dots in Figure 3B). A
190 broad range of genes was significantly altered, with several biological process GO terms
191 significantly enriched in the up-regulated gene list including "response to biotic stimulus" ($p <$
192 $3x10^{-7}$),"response to bacterium" ($p < 3x10^{-7}$) and "defense response" ($p < 3x10^{-7}$). In the down-
193 regulated gene set the GO term most enriched was "sensory perception of chemical stimulus" ($p <$
194 $6x10^{-72}$). The GO molecular functions that were most common in the upregulated sets included
195 enzymes like hydrolases and oxidoreductases, as well as nucleic acid binding genes (Figure 3C).
196 Down-regulated genes include receptors, hydrolases and transporters (Figure 3C).

197 The first tissue that would have contact with airborne volatiles in terrestrial vertebrates are
198 the airways and lungs. We therefore performed transcriptome analyses on lung tissue of mice
199 exposed to diacetyl headspace at different doses for a period of 5 days, as was done in *Drosophila*
200 (Figure 3D). The dose of the volatile in the chamber was measured in parallel experiments by
201 tracking volatile loss and airflow and determined to range between a peak 1920 ppm at the end of
202 hour 2, tapering off to 28 ppm by hour 120 (Supplemental Figure S2B). Indeed, expression of a
203 substantial number of genes was modulated in the diacetyl-exposed lungs compared to the control.
204 The changes were dose-dependent and more pronounced in mice exposed to headspace from a 1%
205 diacetyl source compared to those exposed similarly to 0.1% diacetyl source (Figure 3E,
206 Supplemental Figure S2C). Among these diverse sets of regulated genes in the lung tissue, a
207 significant overlap was found between 1% and 0.1% headspace for both up-regulated genes
208 ($p=3x10^{-3}$) and down-regulated genes ($p=6x10^{-3}$, Figure 4F), further supporting a dose-dependent
209 effect of diacetyl on gene expression in the mouse lung.

The GO enrichment analysis of the lung transcriptome from mice exposed to diacetyl revealed several interesting sets of genes that were significantly altered (Figure 3G,H). Among these genes is the SARS-CoV-2 entry receptor ortholog, ACE2. The level of this gene in the lungs of diacetyl exposed mice showed a reduction in expression levels ($\log_2$ fold-change= - 0.62, FDR= 2.02×10^{-5}). The level of ACE2 in the nasal tissue, lungs and other organs play a critical role in infection by the SARS-CoV-2 virus, suggesting that epigenetic mechanisms may contribute to expression. While we do not know whether expression of ACE2 in humans is regulated similarly, these results highlight the importance of understanding volatile-induced modulation of gene expression in the lungs and other tissues.

HDAC family members are highly conserved across eukaryotes, spanning both animal and insects. Volatile microbial metabolites have been present throughout the evolution of animals, insects, and plants, and have potential as signals for multi-domain communication because they can travel wide ranges; plants detect root infections and time their immune response using volatiles (26), and microbial volatiles elicit olfactory behaviors in insects and nematodes. Our results indicate that a volatile compound, capable of directly inhibiting HDACs and altering acetylation levels, can cause significant changes in gene expression in a variety of organisms following exposure from a distance, through the air.

DEGs overlap those for known HDAC inhibitors and upregulation is partially reversible

One of the hallmarks of epigenetic regulators which makes them attractive candidates for therapeutics is plasticity. Upon removal of the inhibitors, we expect that some of the changes in gene expression are reversible. To test for reversibility, we performed a recovery experiment following diacetyl exposure using the *Drosophila* model. We maintained 5-day diacetyl-exposed

232 flies in clean air for 5 additional days (Figure 4A). In parallel, we performed age-matched mock
233 experiments with paraffin oil solvent exposure alone. A large number of genes were down-
234 regulated following the recovery in comparison to the 10-day-old flies in the mock condition
235 (Figure 4B). Interestingly, there was a significant overlap of these down-regulated genes with the
236 set that was up-regulated in the diacetyl treatment (Figure 4C). These results suggest that the
237 effects of HDAC inhibitory odorant exposure are not permanent but dynamic, and removal of the
238 odorant leads to subsequent changes in gene expression of the up-regulated set.

239 Drugs that inhibit HDACs are in various stages of approval as treatments for several
240 diseases. The approved drugs include sodium butyrate and valproic acid. To compare the gene-
241 regulatory effects of these drugs to diacetyl, we performed RNA-seq after raising the flies on food
242 containing sodium butyrate (SB) or valproic acid (VA) (27) and compared gene expression in the
243 antennae of flies raised on untreated food for 5 days. We next compared the up-regulated gene
244 profiles following each treatment to the one induced by exposure to diacetyl. As expected, feeding
245 SB and VA induced significant changes in expression levels of several genes (Figure 4D,E).
246 Interestingly we found that 113 of diacetyl up-regulated genes were also up-regulated in either SB,
247 VA or both treatment conditions (Figure 4F). Pairwise statistical analysis of each gene set revealed
248 a significant overlap of diacetyl-induced genes with SB-induced genes ($p=6x10^{-11}$) and with VA-
249 induced genes ($p=2x10^{-65}$) (Figure 4F). There was, as expected, also a significant overlap between
250 SB- and VA- induced genes ($p=1x10^{-52}$) (Figure 4F). This highly significant overlap among up-
251 regulated genes lends further support to our model that diacetyl vapors act as an HDAC inhibitor
252 in vivo. As expected, each of the 3 treatments also modulated a substantial number of unique genes
253 (Figure 4G,H), suggesting that differences in molecular structure and activity profile across the
254 repertoire of HDACs may contribute to differences in gene regulation. These results suggest that

some volatile odorants, or the microbes that emit them, may impart therapeutic effects like other HDAC inhibitors from a distance, through the air.

Volatile Diacetyl alters gene expression in the mouse brain

One of the categories of challenging diseases that HDAC inhibitors are being tested for drugs are neurodegenerative diseases (28) where volatile odorants may provide a new class of inhaled therapeutics. A major design challenge for nervous system drugs is the ability to cross the blood-brain barrier. Due to the volatility and small size of volatile odorants, there is a possibility that they could diffuse through the intranasal route to the brain directly (29). We cannot tell *a priori* whether odorants like diacetyl can travel across the nasal membrane to the brain. In order to test whether cells in the brain of mice respond when presented with diacetyl vapors from a distance, we used gene expression as the final readout to measure it. We performed RNA-seq experiments on mice exposed only to aroma of diacetyl in the air for 5 days as before. Littermate controls were exposed in a similar manner to the solvent (PO) in the air. Interestingly, several genes were differentially expressed upon exposure to headspace from 0.1% diacetyl passaged through the air in the holding cage where it is further diluted (49 up-regulated, 32 down regulated, $|\log_2$ fold-change$|$ >1, FDR<0.05) or to headspace from 1% diacetyl diluted in the holding cage (748 up-regulated, 1031 down regulated, $|\log_2$ fold-change$|$ >1, FDR <0.05) (Figure 5B,C). GO analysis of the regulated genes in the exposed mouse brain transcriptome revealed several interesting sets of genes were significantly altered in each set (Figure 5E). These results indicate that a volatile odorant like diacetyl is able to reach the brain in mammals, and presumably alter gene expression in neuronal cells. Although the overall DEG sets are different across the lungs and brain, there is a statistically significant overlap, particularly in the 1% exposure, as would be expected from using the same mechanism of action. There is a highly significant overlap ($p=2x10^{-101}$) between genes

upregulated in the brain compared with the lungs (248 of 748), as well as for downregulated genes ($p=3x10^{-163}$; 477 of 1031 genes) (Figure 5D).

Diacetyl prevents proliferation of neuroblastoma cells

Among the significantly down-regulated genes is *MYCN*, which is known to show increased expression and plays a central role in many types of cancers, suggesting that epigenetic regulation may affect tumor cells. Broad-spectrum HDAC inhibitors have been approved by the FDA for treatment of a variety of cancers. To test the exciting possibility that a volatile HDAC inhibitor, which affects gene expression in the brain, would have an effect against cancers as well, we performed a cell-based assay. We picked neuroblastoma as a candidate since it has a strong dependence on *MYCN* and develop from fetal adrenal neuroblasts (30). Several genetic and "omics" studies have identified genes that are upregulated in neuroblastomas, some of which are considered to key (31). We evaluated the DEGs from the diacetyl-exposed mouse brain transcriptome for several of these key genes. Three of the six key genes identified across multiple studies were significantly altered, two of which were significantly downregulated, *MYCN* (P=2.06E-13, FDR=1.76E-12) and *Alk* (P=3.3E-5, FDR=9.48E-5) (Figure 5F)**.** An unbiased computational study evaluated omics datasets and identified 4 genes that were the best predictors of clinical outcome (32), all of which are significantly different in the brains of the diacetyl exposed mice, strikingly 3 of which were significantly downregulated, *NCAN (p=1.33E-16, FDR=1.59E-15), STK33 (p=4.6E-7, FDR=1.79E-6)* and *ERCC6L2 (p=4.57E-5, FDR=0.00012)* (Figure 5F). These findings are extremely provocative, given that the downregulated genes, particularly MYCN play a role in neuroblastomas and in several other cancers.

We tested diacetyl for the ability to inhibit proliferation of a SH-SY5Y neuroblastoma cell line from a metastatic bone tumor. A significant reduction in cell count was seen in diacetyl treatments in the SH-SY5Y cancer cell cell lines (Figure 5G). In order to validate the initial result, we retested diacetyl with at two concentrations across 3 different cancer cell lines. Diacetyl showed a significant reduction in cell numbers for the neuroblastoma cell line specifically, and not other cell lines, relative to the control (Figure 5G). These results suggest that epigenetic regulation of cancer promoting genes may be caused by exposure to specific volatiles like diacetyl in the environment

Testing therapeutic effect in neuroblastoma and Huntington's neurodegeneration

Since diacetyl is able to affect changes in a mammalian brain by crossing the blood brain barrier, we wanted to test if it can impart therapeutic effects in disorders of the brain like neurodegeneration for which HDAC inhibitors have been proposed as therapeutics. In order to test diacetyl in the context of neurodegenerative disease, we used the well-established *Drosophila* model of Huntington's disease, which has previously been used to demonstrate the efficacy of sodium butyrate in slowing neurodegeneration (27, 33). The human Huntingtin protein with expanded poly-Q repeats is expressed in the neurons of the compound eye in *Drosophila*, causing progressive degeneration of the seven visible photoreceptor rhabdomere cells in each ommatidium (34). We selected this model in particular since polyglutamine disorders are well suited for targeting by inhibitors of HDAC1 and HDAC3 (35) such as diacetyl (Figure 1B). Moreover, previous studies have shown that orally administered HDAC inhibitors such as sodium butyrate and SAHA can significantly reduce photoreceptor degeneration in this model (27). When the transgenic flies expressing two copies of the human Huntingtin with poly-Q repeats (HTTQ120) under control of the eye-specific GMR promoter were raised at 18°C, the number of rhabdomeres

322 in each ommatidium was similar to that normally observed in wild-type flies immediately post-
323 eclosion (day 1, Figures 6A-C). When these HTTQ120 flies were moved to 25° C following
324 eclosion (Figure 6A), they showed dramatic degeneration of rhabdomeres over a period of 10 days
325 (Figures 6B, D-G). The mean number of rhabdomeres was reduced from 7 to ~1 by day 10. The
326 dose of the volatile in the chamber was measured in parallel experiments by tracking volatile loss
327 and airflow (0.5 L/min) and determined to range from 260-95 ppm, an average of 125 ppm at the
328 end of hour 1, tapering off to 0 ppm by hour 24. The odorant was replaced each day, leading to a
329 dosage profile that appears like a once a day pill (Supplemental Figure S1A).

330 Remarkably, when the Huntingtin (HTTQ120)-expressing flies were exposed immediately
331 after eclosion to volatile headspace of 1% diacetyl (Figure 6A), they showed a substantial (~50%)
332 reduction of rhabdomere loss (Figures 6B, D-G). The majority of ommatidia retained 6-7
333 rhabdomeres at day 5 (Figures 6D and F). Even after 10 days, the majority of the omamtidia still
334 had 2-3 rhabdomeres left in the odor-exposed flies, while the solvent controls had only ~1-2
335 rhabdomeres (Figures 6E and G). These results demonstrate that exposure to volatile diacetyl in
336 air slows down the photoreceptor degeneration caused in these Huntington's disease model flies.
337 Thus, odorants like diacetyl may have potential as a prophylactic against this neurodegenerative
338 disorder. Therefore, the volatile odorant can both significantly alter gene expression from a
339 distance as well as cause a phenotypic change in the fly with a human disease gene.

340 **Discussion**

341 In this study, we discovered that eukaryotic cells have the ability to alter gene expression
342 in response to an odorant, in a manner independent of traditional neuronal activity-induced
343 pathways. Members of a conserved family of HDACs detect the concentration of diacetyl

344 differentially. Diacetyl exposure increased levels of H3K9 acetylation in the nucleus in a dose-
345 dependent manner, and leads to changes in gene expression. The odorant diacetyl occurs naturally
346 and is generated from the metabolism of a variety of food components, including triglycerides,
347 sugars and amino acids (5). Moreover, the chemical is produced by the activity of microorganisms
348 such as yeasts and lactic bacteria during fermentation in many foods and beverages (5). Although
349 beyond the scope of this study, the discovery that cells can alter gene expression upon prolonged
350 exposure to a common naturally occurring odorant raises important questions about the potential
351 physiological consequences of the expression changes. Given our repeated exposure to particular
352 flavors and fragrances, the findings outlined here highlight a new consideration for evaluating the
353 safety of certain volatile chemicals that can cross the cell membrane.

354 In mammals, up-regulation of circulating β-hydroxybutyrate during fasting or calorie
355 restriction induces changes in the expression of a set of genes (21). The acetylation mark specificity
356 and IC_{50} of β-hydroxybutyrate is similar to that of diacetyl. Any beneficial physiological effects
357 of odor-detection at lower odor concentrations would also be countered by studies of potential
358 risks at higher concentrations. In fact, the deleterious effect of exposure to high levels to diacetyl
359 causing bronchiolitis obliterans, or "popcorn lung", and its toxicity in cultured cells is already
360 known (36). Even so it is present in several foods we eat and is on the GRAS (Generally Regarded
361 as Safe) list of Flavor and Extract Manufacturers Association (FEMA) for use as a flavoring
362 ingredient at low concentrations. While the specific mechanism of "popcorn lung" is unknown, it
363 has previously been proposed that carbonyl groups of diacetyl can react to modify amino acid side
364 chains on proteins or generate reactive dicarbonyl and reactive oxygen species, leading to
365 excessive cytokine production and inflammation (37). Our results raise the possibility that the
366 molecular mechanisms underlying this disorder could also be partially attributed to the unusually

high HDAC-mediated genetic response to diacetyl by cells in the lungs. Several studies using rodent animal models have shown toxicity of high levels of diacetyl in the respiratory tracts including the nose and lungs (38, 39). The toxic effect of higher dosages has been observed for many types of HDAC inhibitors. For example, in one *Drosophila* study, feeding of a high dosage of 4-phenylbutyrate reduces survival rate, while a lower dosage extends longevity (40). Another concern is that one of the highest known levels of diacetyl exposure to humans, however, is through smoking cigarettes, where exposure from even a single cigarette (250-361ppm) is high (41, 42): Salem (128 μg/cigarette), Camel (128.1 μg/cigarette), Carlton (45.6 μg/cigarette) (42). Different types of diets and lifestyle choices have been known to have effects on health and well-being due to differences in balance of different health promoting ingredients, yet little is known about role of such flavors, fragrances and metabolites acting on epigenetic marks and altering gene expression. Our findings raise the possibility that diacetyl and structurally related odors in the environment may affect gene expression directly through absorption/transport into these cells. In mammals, the epithelium-lined lungs and nasal/oral pathway is directly exposed to odorants presenting an opportunity to affect gene expression and physiology.

Eukaryotes primarily detect volatile odorants in the environment using olfactory neurons that express a variety of transmembrane receptors, a family of genes that have independently evolved multiple times in different phyla. Examples of these unrelated genes include: the ionotropic 7-transmembrane (TM) odorant receptor *(*Or*)* family, which is insect-specific; 3-TM ionotropic receptors (IRs), which are present across most arthropods; the nematode-divergent 7-TM GPCRs belonging to the *str, sra, srg, srw, srz, srbc, srsx* and *srr* families; the mammalian 7-TM GPCR olfactory receptor (OR) family; and the trace amine-associated receptor (TAAR) family (43-47). The activation of these receptors induces neuronal action potentials, and this information

390 is conveyed to higher brain centers where olfactory perception is generated (48). This second
391 response pathway which we have discovered is much slower and has an enzymatic mechanism
392 which draws parallels with the multiple pathways in place to detect light. In the specialized cells
393 of the eye, detection of light occurs via rhodopsins (7-transmembrane GPCRs) and leads to
394 neuronal activity and behavioral responses. However, other cells, including in plants, are also able
395 to respond to changes in light intensity of certain wavelengths using the ancient, conserved
396 cryptochrome proteins that are related to photolyases (49). This suggests that vital sensory
397 modalities can be detected via multiple pathways. Our observations raise the question whether
398 HDACs represent a conserved detection mechanism for odorants like diacetyl that link odor-
399 detection to a specific gene expression response. HDAC proteins, however, are an ancient family
400 of genes that predate even histones themselves (50, 51). It is conceivable that odor detection
401 mechanisms that emerged in ancient forms may not have involved specialized transmembrane
402 receptors, or neurons, or resulted in rapid behavioral movements.

403 Our data suggests that an HDAC inhibitory odorant also affects gene expression in the lungs
404 and brain of mice, including significantly decreasing the expression level of the ACE2 receptor,
405 whose ortholog in humans is the entry receptor for the SARS-CoV-2 virus that causes Covid-19.
406 The applied impact for the future could be far-reaching, as HDACs are known to affect a wide
407 variety of pathways in eukaryotes, and inhibitors are candidates for novel inhaled therapeutics as
408 treatment of many conditions such as Covid-19, cancers, neurodegeneration and a variety of
409 infectious diseases (52-60).

410 Our studies also show that one of the volatiles is protective against the neurodegenerative
411 effects of Huntington's and neuroblastoma. This new class of chemicals will allow us to
412 understand how our environment, diet and microbiome shapes the epigenetic landscape in the

lungs and affects inflammation and immune responses. Our strategy to investigate consequences in model systems will lay a comprehensive groundwork for future research, but also allow identification of key molecular biomarkers that can be associated with observation of epigenetic effects, toxic or not, in individuals. The public health impact of these findings will be far-reaching, both from the perspective of toxicity as well as therapeutics. Investigating the health safety concerns of exposure to such odorants at high doses or prolonged periods is essential to understand potential for damage. Conversely, at non-toxic concentrations HDAC inhibitors can be used for treatment of many debilitating conditions in the lungs such as COPD, inflammation, and Covid-19 infection (61). Taken together, our discovery that cells can alter gene expression in response to an odor that acts as an HDAC inhibitor and reprogram gene expression, promises the pursuit of new types of odor-based therapeutics already approved for human consumption as prophylactics for a myriad of diseases. Simultaneously, they raise the concern of a new type of environmental agent which can reprogram gene expression and have widespread effects that are yet unknown.

METHODS

Drosophila Stocks and Manipulations

Fly stocks were maintained on conventional fly food under a 12-hr. light:12 hr. dark cycle at 18°C or 25°C. The fly strain of *w1118* backcrossed 5 times to *Canton-S* (*wCS*) was used in all the *Drosophila* transcriptome experiments. P{GMR-HTT.Q120}2.4 (Bloomington # 8533) were used for neurodegeneration experiments. For imaging *Gr63a-Gal4; UAS-mcd8:GFP, Gr21a-Gal4; UAS-mcd8:GFP* stocks were obtained as a kind gift from the Carlson lab, Yale.

Odor exposure experiments for imaging

436 Newly eclosed male wCS flies were sorted in groups of 30 into vials with standard cornmeal medium.
437 Vials were closed with two overlapping 3''x3''polypropylene mesh squares and tied with cotton twine.
438 Vials were used within 6 hours. Four vials were placed in a 1000ml Nalgene straight sided jar with a
439 10ml glass beaker with 10ml of diacetyl 10^{-2} in paraffin oil. Jars were closed for exposure periods
440 ranging from 2-6 days. In recovery experiments, vials were removed from the jars and were placed in a
441 25°C incubator for the remainder of the recovery period. Flies were anesthetized on ice, sacrificed in
442 ethanol, and then immediately put into 1X phosphate buffered saline with 0.3% triton-x (PTX). Brains or
443 antenna were put in 4% paraformaldehyde in PTX and incubated for 30min while rotating at 25°C.
444 Samples were washed 5 times in PTX, and blocked in 5% natural goat serum in PTX for 1 hr while
445 rotating at 25°C. Samples were then incubated in primary antibody with 5% goat serum in PTX, mouse-
446 nc82 (1:20) (Development Studies Hybridoma Bank, University of Iowa) and rabbit-antiGFP (1:150)
447 (Invitrogen) in PTX for 48 hours in 4°C while rotating. After washing 5 times in PTX samples were
448 incubated in secondary antibody with 5% goat serum in PTX, rabbit-anti-Alexa488 (1:400) (Invitrogen)
449 and mouse-antiAlexa568 (1:400) (Invirtogen) for 48 hours in 4°C. Samples are washed 5 times in PTX
450 and stored in 70% glycerol in PTX. Images were taken using a Ziess 510 laser scanning confocal
451 microscope, and image analysis was done using Image J software.

452 **QRT-PCR**

453 Drosophila heads (with antenna) were collected on liquid nitrogen and stored at -80°C until processing.
454 300 heads were collected for each sample, and ground on liquid nitrogen. mRNA was extracted using a
455 PolyATract kit (Promega), and was reverse transcribed using Superscript III (Invitrogen) according to the
456 manufacturer's protocol. The quality of the cDNA was assessed on a 1.5% agarose gel. cDNA was
457 added to individual reactions of SYBR green master mix (BioRad) and run on a BioRad-MyQ
458 thermocycler. The program began with a single cycle for 3-min at 95°C, followed by 40 cycles of 15-sec
459 at 95°C, 30-sec at 58°C and 30-sec at 72°C. Afterward, the PCR products were heated to 95°C for 1-min,
460 and cooled to 55°C for 1-min, to measure the dissociation curves. The efficiency of each primer set was

first validated by constructing a standard curve and three 10x serial dilutions of first strand cDNA. For each serial dilution, the CT value was plotted against the log (template dilution) and the slope and r^2 value of each regression line calculated. Expression of each *Or* or *Gr* gene was assessed in triplicate. Dissociation curves were used to assess the purity of the PCR reactions. *Or* and *Gr* transcript levels were normalized by using the transcript levels of *ribosomal protein 49*. Expression levels were calculated using the Pfaffl equation.

In general, primers were designed by using coding sequences close to the 3' end of the gene, and where possible, primers spanned an intron.

Primers:

Gr21a F: CGATCGTCTTTCCGAATCTC

Gr21a R: GGCTCAGATCCACCCATAGA

Gr63a F: AAATGAACTCCGCCTCCTTT

Gr63a R: CGCAATTTCAGAGGCAAACT

RP49 F: CTGCCCACCGGATTCAAG

RP49 R: GTTTCATGCGGCGAGATCG

Or47a F: ATCACAGGCCACATTGAACA

Or47a R: TCCCCGCAGTAGCAGTAGAT

Or88a F: TTAAAGTGGCCTTCCTGGTG

Or88a R: ATGCGGCAATAAAGTTCCAC

Or83b F: TTCTTGGCATTCGCTTTTCT

481 Or83b R: TCCCTGGATTTGTTTGCTTC

482 **Odor Exposure Protocol for Transcriptome Analysis**

483 Flies were exposed to diacetyl (B85307, Sigma-Aldrich, St. Louis, MO) by placing them in vials
484 in a cylindrical closed container (112 mm diameter x 151 mm height) along with an odor-
485 containing glass vial. The odorant was dissolved in 5 mL paraffin oil at 1% dilution. For a given
486 exposure protocol, two groups of flies were prepared: those exposed to 1% diacetyl headspace and
487 those exposed to paraffin oil headspace alone (control flies). Adult male flies aged 1 d were
488 transferred to fly vials containing fresh medium and put into the container with the odor vial. At
489 the end of the fifth day of exposure, flies were collected, and their antennae were dissected for
490 RNA extraction. All treatments and experiments were performed at room temperature. For the
491 recovery experiment, flies were transferred to a container with a glass vial of paraffin oil after 5
492 days of diacetyl exposure. At the end of the fifth day of recovery, flies were collected, and their
493 antennae were dissected for total RNA extraction. The second and third antennal segments from
494 40-60 male flies after treatment were carefully hand-dissected from the head and collected in 1.5
495 ml microfuge tubes kept cold in liquid nitrogen. Antennae were mechanically crushed with
496 disposable RNAse-free plastic pestles, and total RNA was isolated using a Trizol-based protocol.
497 cDNA libraries were prepared from total RNA using the Illumina TruSeq RNA Sample
498 Preparation Kit (v2) and 50 bps single- and paired-end sequencing was done using the
499 HighSeq2000. Two biological replicates were sequenced for each condition, with an average of
500 27 million reads / replicate, and with an average of 84% mapped.

501 Two-month old C57BL/6 male mice (2-3 for each condition in a single cage) were
502 continually exposed to air flowing over headspace of paraffin oil (solvent control), 0.1%, or 1%

503 diacetyl over a period of 5 days, then euthanized for collecting the lung and brain tissues and
504 processing for mRNA isolation. All protocols for animal use and euthanasia were approved by the
505 Institutional Animal Care and Use Committee (#20150028) and were in accordance with the
506 provisions established by the Animal Welfare Act and the Public Health Services (PHS) Policy.
507 In the transcriptome analysis, two replicates were performed for each condition, with an average
508 of 123,687,411 reads / replicate, with an average of 88% mapped. Multiplexed libraries were
509 made from total RNA input using the Illumina TruSeq RNA sample preparation kit (v2) and 50
510 bps single-end sequencing was done using the NextSeq500.

511 **Calculation ppm in air based on weight loss of odorant over time**

512 The odor solution in PO in each setup (Drosophila and mouse) was weighed using a sensitive
513 balance. PO is non-volatile and therefore weight loss is attributable to diacetyl volatilization.
514 Volatile Headspace exposure (ppm) is calculated through odor cartridge weight change from pure
515 odor compound volatizing out (Inamdar et al., 2012).

516 $ppm=(10^6\ w/MW)/(v/V_m)$

517 Where ppm is the concentration of tested VOC in parts per million (v/v); w is the weight of the
518 tested chemical in grams; MW is the molecular weight of the tested VOC (grams/mole); v is the
519 total volume of the respective exposure chambers; and Vm is the molecular volume under the
520 tested condition.

521 •$V_m=24.45(760/P)((t+273.15)/298.15)$

522 Where 24.45 = gram molecular volume, under standard Lab conditions of 760 mm Hg, 25°C; P =
523 ambient pressure, in mm Hg; and t = ambient temperature, in °C. Odor cartridges, consisting of

varying odor volume/volume dilutions, were weighed periodically under standard ambient temperature and pressure. Under these conditions, the pure volatile odor compounds volatize out of the odor cartridge and the evaporation rates were used for our exposure calculations. Based on Ideal Gas Law and experimental conditions, ppm is calculated based on volatized odor compound and experimental chamber volume based on airflow.

HDAC inhibitor Treatment Protocol for Transcriptome Analysis

Sodium butyrate (B5887, Sigma-Aldrich) or valproic acid (P4543, Sigma-Aldrich) were dissolved in normal fly food medium at the final concentration of 10 mM. Three groups of flies were prepared: those treated with one of the HDAC inhibitors and those without HDAC inhibitor treatment (control flies). Adult flies aged 1 d were transferred to fly vials containing medium with or without a HDAC inhibitor. At the end of the fifth day of treatment, flies were collected, and their antennae were dissected for RNA extraction. All treatments and experiments were performed at room temperature. Two biological replicates with 60 flies/replicate were performed for each condition, with an average of 23 million reads / replicate, and with an average of 92% mapped. Multiplexed libraries were made from total RNA input using the Illumina TruSeq RNA sample preparation kit (v2) and 50 bps paired-end sequencing was done using the HighSeq2000.

Bioinformatic analysis of RNA-seq experiments

Reads aligned to the latest release of each of the genomes used (dm6 for the *Drosophila* genome, GRCm38 for the *Mus Musculus* genome) and quantified with kallisto (version 0.43.1) (62) Only libraries for which we obtained >75 % alignment were used for downstream analysis. Transcript counts were summarized to gene-level using tximport package (version 1.4.0)(63). For any instances of detected batch effects, we removed unwanted variation using RuvR in the RuvSeq

546 package (version 1.10.0)(64). Differentially expressed gene (DEG) analysis was performed with
547 the edgeR package (version 3.18.1)(65) using low count filtering (cpm >0.5) and TMM
548 normalization. Protein classification analysis was performed with PANTHER (version 13.1)(66).
549 All significance analyses of gene overlap were done using the GeneOverlap package in R package
550 (version 1.14.0). GO enrichment analysis was performed using clusterProfiler (version 3.6.0)(67).

551 **HDAC Activity Assays**

552 HDAC activity of class I HDACs (HDAC1, 2, 3 and 8) was measured with the fluorometric HDAC
553 Activity Assay kit: HDAC1 (10011563, Cayman Chemical, Ann Arbor, MI), HDAC2, HDAC 3,
554 and HDAC 8 (50062, 50073 and 50068, BPS Bioscience, San Diego, CA), according to the
555 manufacturer's instructions. HDAC activity of class II HDACs (HDAC4 and HDAC6) were
556 measured with the fluorometric HDAC Activity Assay kit: HDAC4, HDAC 4 (50064 and 50076,
557 BPS Bioscience, San Diego, CA), according to the manufacturer's instructions.
558 Due to interference, concentrations of >30 mM were not used in the IC50 calculation. To account
559 for any interference at lower concentrations, all baseline measurements of blank wells (no HDAC
560 enzyme) were performed and subtracted with the various concentrations of diacetyl.

561 **Cell Culture and Treatment**

562 Human embryonic kidney 293 (HEK293) cells were grown in 100 mm cell culture dishes with
563 Dulbecco's modified Eagle's medium (DMEM) (10-013, Corning, Manassas, VA), supplemented
564 with 10% fetal bovine serum (FBS) (26140-079, Gibco, Carlsbad, CA) at 37°C with 5% CO_2.
565 Cells that were ~80% confluent were treated with freshly prepared medium supplemented with
566 diacetyl at concentrations indicated. The cells for mock controls were handled in the same manner
567 without adding diacetyl to the medium. In order to prevent diffusion of diacetyl odor from the

568 treatment dishes to the ones of mock control, the cell culture dishes in different conditions were
569 cultured in separate CO_2 incubators.

570 Cell proliferation assays were performed to assess effects of compounds against cancer cell lines.
571 Cells were maintained in a 37°C incubator with 5% CO_2 throughout the whole experiment.
572 Compound stocks are dissolved in 10% DMSO, and final concentrations made fresh in complete
573 media as needed. 10% DMSO solvent is used as control in complete media. Cells were seeded
574 onto 12-well plates and allowed 12-24 hours until treatment to allow cells to adhere to wells.
575 This is followed by minimum 5-day treatment of compounds, changing the media with treatment
576 every 48 hours. Cell lines A549, PC3, and SK-MEL-5 will be seeded at 8000 cells/well, which
577 was determined to provided 80-100% confluency after 6-day growth. SH-SY5Y was seeded at
578 8000 cells/well and 16,000 cells/well due to their known slower division rate and given at least
579 10 days for sufficient growth. After allotted growth times, cell counts were performed using the
580 CountessTM automated cell counter. All assays had a minimum of three replicates for all
581 conditions and analyzed through GraphPad Prism One-way ANOVA for significance.

582 **Odor Exposure Protocol for Huntington's Disease Model Flies**

583 Flies were exposed to diacetyl in a cylindrical container (112 mm diameter x 151 mm height).
584 Each container was tightly closed but had 2 holes, one of which connected to an air suction port,
585 and the other to a vial containing either of 5 mL paraffin oil or 5 mL 1% diacetyl in paraffin oil. A
586 gentle suction was applied to pull the headspace from the odor or paraffin oil vials into the
587 cylindrical structure. pGMR-HTTQ120 flies were maintained at 18°C. Adult flies aged 1 d were
588 transferred to fly vials containing fresh medium and put into the odor-filled container at room
589 temperature. Paraffin oil and 1% diacetyl solution were prepared and replaced every day. At the

590 end of the fifth day of exposure, half of the flies were collected and subjected to pseudopupil
591 analysis as before (27). The remaining flies were transferred to fresh medium and exposed to the
592 odors for an additional 5 days. All treatments and experiments were performed at room
593 temperature. The number of rhabdomeres in each ommatidium was counted using the pseudopupil
594 analysis, and statistical significance was determined by unpaired t test (two-tailed) against PO at
595 each time point.

596 **Preparation of Nuclear Extracts from HEK293 Cells**

597 Nuclear extracts of HEK293 cells were prepared according to a protocol described previously (68),
598 with minor modifications. In brief, HEK293 cells were washed twice with cold phosphate-buffered
599 saline (PBS) and lysed with hypotonic buffer (10 mM HEPES-KOH [pH 7.9], 1.5 mM $MgCl_2$, 10
600 mM KCl, protease inhibitor cocktail (04693159001, Roche, Indianapolis, IN), 1 mM DTT, 1 mM
601 TSA). Following a brief centrifugation, the pellet was resuspended in hypertonic buffer (20 mM
602 HEPES-KOH [pH 7.9], 25% glycerol, 420 mM NaCl 1.5 mM $MgCl_2$, 0.2 mM EDTA, protease
603 inhibitor cocktail, 1 mM DTT, 1 mM TSA). The supernatant was recovered as nuclear extract.

604 **Western Blot Analysis**

605 Proteins in the nuclear extracts (60 μg protein) were separated by SDS–PAGE gels (456-1043,
606 Bio-Rad, Hercules, CA), transferred onto PVDF membranes (162-0174, Bio-Rad), and incubated
607 with anti-histone antibodies: acetylated H3K9 (1/2000: ab4441, abcam, Cambridge, MA),
608 acetylated H3K14 (1/5000: 06-911, EMD Millipore, Billerica, MA), acetylated H4K5 (1/2000:
609 07-327, EMD Millipore). Bound antibody was detected by horseradish peroxidase-conjugated
610 anti-rabbit secondary antibody (1/20000: 1705046, Bio-Rad) and developed using Clarity™
611 Western ECL Substrate (1705060, Bio-Rad). Signals were detected and captured by

612 ImageQuant™ LAS 4000 mini (GE healthcare, Pittsburgh, PA), and band intensities were
613 quantified with ImageJ software. H3K9 acetylation intensity in individual lanes was reported
614 relative to the normalized Mock treatment, and calculated using this formula: Relative H3K9ace
615 intensity for each timepoint = (H3K9ace / PCNA) / averaged (Mock H3K9ace / Mock PCNA).
616 Statistical significance was determined by unpaired *t* test (two-tailed) against mock at each time
617 point.

618 **Data availability**

619 All transcriptome data sets in this publication have been deposited in the GEO repository
620 with accession number GSE116502. All other data is presented in the figures, tables and
621 supplementary materials.

622 **Author contributions:** S. H.Y. performed the biochemical assays, cell culture assays,
623 neurodegeneration assays and wrote the first draft. R.N.F performed biochemical assays and the
624 cancer cell line exposure experiments and helped write the paper. C.A.S performed the
625 bioinformatics and transcriptome analysis, parts of the biochemical assays, and helped write the
626 paper. S.P. performed some of the transcriptome analysis. S.T.C performed the imaging studies
627 and RT-PCR. C.P. performed some biochemical analyses. M.G.N. helped plan and assisted with
628 the mouse exposure experiments. A.R. conceptualized the study, planned and supervised the
629 experiments and wrote the final draft of the paper.

630 **Competing interests:** A.R. is founder of startups: Sensorygen working on computational
631 neurobiology of olfaction and taste, and Remote Epigenetics working on small molecule
632 enhancement of agricultural production. A.R., S.T.C., S.H.Y., R.N-F., are listed as inventors on
633 patents filed by University of California.

Acknowledgments: We would like to thank Dr. Larry Marsh for advice about the fly eye assay and HDAC inhibitors, Joel Kowalewski for help with critical comments, Dr. Thomas Girke for guidance in bioinformatics analysis, Drs. Anupama Dahanukar, Naoki Yamanaka, Chih-cheng Tsai, Karine Le Roch and Adler R. Dillman for sharing equipment and reagents. This work was partially supported by funds provided by the National Institutes of Health, NIAID (R01AI153195 to M.G.N and R01AI087785 to A.R), and HATCH funds from the Agricultural Experimentation Station UC Riverside to A.R.

References

1. McFall-Ngai M, *et al.* (2013) Animals in a bacterial world, a new imperative for the life sciences. *Proceedings of the National Academy of Sciences* 110(9):3229-3236 %U http://www.pnas.org/content/3110/3229/3229.
2. Dorrestein PC, Mazmanian SK, & Knight R (2014) Finding the missing links among metabolites, microbes, and the host. *Immunity* 40(6):824-832.
3. Wikoff WR, *et al.* (2009) Metabolomics analysis reveals large effects of gut microflora on mammalian blood metabolites. *Proceedings of the National Academy of Sciences* 106(10):3698-3703 %U http://www.pnas.org/content/3106/3610/3698.
4. Rooks MG & Garrett WS (2016) Gut microbiota, metabolites and host immunity. *Nat Rev Immunol* 16(6):341-352.
5. Shibamoto T (2014) Diacetyl: occurrence, analysis, and toxicity. *J Agric Food Chem* 62(18):4048-4053.
6. Devaud JM, Acebes A, & Ferrus A (2001) Odor exposure causes central adaptation and morphological changes in selected olfactory glomeruli in Drosophila. *Journal of Neuroscience* 21(16):6274-6282.
7. Sachse S, *et al.* (2007) Activity-dependent plasticity in an olfactory circuit. *Neuron* 56(5):838-850.
8. Devaud JM, Acebes A, & Ferrus A (2001) Odor exposure causes central adaptation and morphological changes in selected olfactory glomeruli in Drosophila. *J Neurosci* 21(16):6274-6282.
9. Martineau B, Henick-Kling, T., Acree, T. (1995) Reassessment of the Influence of Malolactic Fermentation on the Concentration of Diacetyl in Wines. *Am J Enol Vitic* 46(3):385-388.
10. Nykanen L, Nykanen, I. (1991) Distilled beverages. *Volatile Compounds in Foods and Beverages*, ed Maarse H (Dekker Inc, New York), pp 548-580.
11. Hughes PS, Baxter, E.D. (2001) Flavour Determinants of Beer Quality. *Beer: Quality, Safety and Nutritional Aspects*, (The Royal Society od Chemistry, Camdridge, UK), pp 40-73.

12. Turner SL & Ray A (2009) Modification of CO2 avoidance behaviour in Drosophila by inhibitory odorants. *Nature* 461(7261):277-281.
13. Shahbazian MD & Grunstein M (2007) Functions of site-specific histone acetylation and deacetylation. *Annu Rev Biochem* 76:75-100.
14. Graff J & Tsai LH (2013) Histone acetylation: molecular mnemonics on the chromatin. *Nat Rev Neurosci* 14(2):97-111.
15. Minucci S & Pelicci PG (2006) Histone deacetylase inhibitors and the promise of epigenetic (and more) treatments for cancer. *Nat Rev Cancer* 6(1):38-51.
16. Kazantsev AG & Thompson LM (2008) Therapeutic application of histone deacetylase inhibitors for central nervous system disorders. *Nat Rev Drug Discov* 7(10):854-868.
17. Chuang DM, Leng Y, Marinova Z, Kim HJ, & Chiu CT (2009) Multiple roles of HDAC inhibition in neurodegenerative conditions. *Trends Neurosci* 32(11):591-601.
18. Jones WD, Cayirlioglu P, Kadow IG, & Vosshall LB (2007) Two chemosensory receptors together mediate carbon dioxide detection in Drosophila. *Nature* 445:86-90.
19. Berdnik D, Chihara T, Couto A, & Luo L (2006) Wiring Stability of the Adult Drosophila Olfactory Circuit after Lesion. *J. Neurosci.* 26(13):3367-3376.
20. Sigg D, Thompson CM, & Mercer AR (1997) Activity-Dependent Changes to the Brain and Behavior of the Honey Bee, Apis mellifera (L.). *J. Neurosci.* 17(18):7148-7156.
21. Shimazu T, *et al.* (2013) Suppression of oxidative stress by beta-hydroxybutyrate, an endogenous histone deacetylase inhibitor. *Science* 339(6116):211-214.
22. Whiteson KL, *et al.* (2014) Breath gas metabolites and bacterial metagenomes from cystic fibrosis airways indicate active pH neutral 2,3-butanedione fermentation. *ISME J* 8(6):1247-1258.
23. Krogerus K & Gibson BR (2013) Influence of valine and other amino acids on total diacetyl and 2,3-pentanedione levels during fermentation of brewer's wort. *Appl Microbiol Biotechnol* 97(15):6919-6930.
24. Krautkramer KA, Rey FE, & JM. D (2017) Chemical signaling between gut microbiota and host chromatin: What is your gut really saying? . *J Biol Chem* 292(21):8582-8593.
25. James A, Austin C, Cox D, Taylor D, & Calvert R (2013) Microbiological and biochemical origins of human axillary odour. *FEMS Microbiol Ecol* 83(3):527-540.
26. Effantin G, Rivasseau C, Gromova M, Bligny R, & Hugouvieux-Cotte-Pattat N (2011) Massive production of butanediol during plant infection by phytopathogenic bacteria of the genera Dickeya and Pectobacterium. *Molecular microbiology* 82(4):988-997.
27. Steffan JS, *et al.* (2001) Histone deacetylase inhibitors arrest polyglutamine-dependent neurodegeneration in Drosophila. *Nature* 413(6857):739-743.
28. Fischer A (2010) [HDAC inhibitors as therapy for neural disorders. Discovery of a new therapy]. *Pharm Unserer Zeit* 39(3):204-209.
29. Chauhan MB & Chauhan NB (2015) Brain Uptake of Neurotherapeutics after Intranasal versus Intraperitoneal Delivery in Mice. *J Neurol Neurosurg* 2(1).
30. Jansky S, *et al.* (2021) Single-cell transcriptomic analyses provide insights into the developmental origins of neuroblastoma. *Nature Genetics* 53(5):683-693.
31. Pugh TJ, *et al.* (2013) The genetic landscape of high-risk neuroblastoma. *Nature Genetics* 45(3):279-284.
32. Zhong X, *et al.* (2018) Identification of Potential Prognostic Genes for Neuroblastoma. *Front Genet* 9.
33. Marsh JL & Thompson LM (2006) Drosophila in the study of neurodegenerative disease. *Neuron* 52(1):169-178.
34. Jackson GR, *et al.* (1998) Polyglutamine-expanded human huntingtin transgenes induce degeneration of Drosophila photoreceptor neurons. *Neuron* 21(3):633-642.
35. Thomas EA (2014) Involvement of HDAC1 and HDAC3 in the Pathology of Polyglutamine Disorders: Therapeutic Implications for Selective HDAC1/HDAC3 Inhibitors. *Pharmaceuticals (Basel)* 7(6):634-661.

36. More SS, Raza A, & Vince R (2012) The butter flavorant, diacetyl, forms a covalent adduct with 2-deoxyguanosine, uncoils DNA, and leads to cell death. *J Agric Food Chem* 60(12):3311-3317.
37. Starek-Swiechowicz B & Starek A (2014) Diacetyl exposure as a pneumotoxic factor: a review. *Rocz Panstw Zakl Hig* 65(2):87-92.
38. Morgan DL, Flake GP, Kirby PJ, & Palmer SM (2008) Respiratory toxicity of diacetyl in C57BL/6 mice. *Toxicol Sci* 103(1):169-180.
39. Palmer SM*, et al.* (2011) Severe airway epithelial injury, aberrant repair and bronchiolitis obliterans develops after diacetyl instillation in rats. *PLoS One* 6(3):e17644.
40. Kang HL, Benzer S, & Min KT (2002) Life extension in Drosophila by feeding a drug. *Proc Natl Acad Sci U S A* 99(2):838-843.
41. Rigler MW & Longo WE (2010) Emission of diacetyl (2,3 butanedione) from natural butter, microwave popcorn butter flavor powder, paste, and liquid products. *Int J Occup Environ Health* 16(3):291-302.
42. Pierce JS, Abelmann A, Spicer LJ, Adams RE, & Finley BL (2014) Diacetyl and 2,3-pentanedione exposures associated with cigarette smoking: implications for risk assessment of food and flavoring workers. *Crit Rev Toxicol* 44(5):420-435.
43. Buck L & Axel R (1991) A Novel Multigene Family May Encode Odorant Receptors: A Molecular Basis for Odor Recognition. *Cell* 65:175-187.
44. Clyne PJ*, et al.* (1999) A novel family of divergent seven-transmembrane proteins: candidate odorant receptors in *Drosophila*. *Neuron* 22(2):327-338.
45. Troemel ER, Chou JH, Dwyer ND, Colbert HA, & Bargmann CI (1995) Divergent seven transmembrane receptors are candidate chemosensory receptors in *C. elegans*. *Cell* 83(2):207-218.
46. Benton R, Vannice K, Gomezdiaz C, & Vosshall L (2009) Variant Ionotropic Glutamate Receptors as Chemosensory Receptors in Drosophila. *Cell* 136(1):149-162.
47. Vosshall LB, Amrein H, Morozov PS, Rzhetsky A, & Axel R (1999) A spatial map of olfactory receptor expression in the *Drosophila* antenna. *Cell* 96(5):725-736.
48. Knaden M & Hansson BS (2014) Mapping odor valence in the brain of flies and mice. *Curr Opin Neurobiol* 24(1):34-38.
49. Fogle KJ*, et al.* (2015) CRYPTOCHROME-mediated phototransduction by modulation of the potassium ion channel beta-subunit redox sensor. *Proc Natl Acad Sci U S A* 112(7):2245-2250.
50. Gregoretti IV, Lee YM, & Goodson HV (2004) Molecular evolution of the histone deacetylase family: functional implications of phylogenetic analysis. *J Mol Biol* 338(1):17-31.
51. Postberg J, Forcob S, Chang WJ, & Lipps HJ (2010) The evolutionary history of histone H3 suggests a deep eukaryotic root of chromatin modifying mechanisms. *BMC Evol Biol* 10:259.
52. Witt O & Lindemann R (2009) HDAC inhibitors: magic bullets, dirty drugs or just another targeted therapy. *Cancer Lett* 280(2):123-124.
53. Wang J*, et al.* (2013) Potential advantages of CUDC-101, a multitargeted HDAC, EGFR, and HER2 inhibitor, in treating drug resistance and preventing cancer cell migration and invasion. *Mol Cancer Ther* 12(6):925-936.
54. Wang J*, et al.* (2012) Sirtinol, a class III HDAC inhibitor, induces apoptotic and autophagic cell death in MCF-7 human breast cancer cells. *Int J Oncol* 41(3):1101-1109.
55. Yeung A*, et al.* (2012) HDAC inhibitor M344 suppresses MCF-7 breast cancer cell proliferation. *Biomed Pharmacother* 66(3):232-236.
56. Park JH*, et al.* (2012) A new synthetic HDAC inhibitor, MHY218, induces apoptosis or autophagy-related cell death in tamoxifen-resistant MCF-7 breast cancer cells. *Invest New Drugs* 30(5):1887-1898.
57. Cai X*, et al.* (2010) Discovery of 7-(4-(3-ethynylphenylamino)-7-methoxyquinazolin-6-yloxy)-N-hydroxyheptanamide (CUDc-101) as a potent multi-acting HDAC, EGFR, and HER2 inhibitor for the treatment of cancer. *J Med Chem* 53(5):2000-2009.

58. Shankar S & Srivastava RK (2008) Histone deacetylase inhibitors: mechanisms and clinical significance in cancer: HDAC inhibitor-induced apoptosis. *Adv Exp Med Biol* 615:261-298.
59. Platta CS, Greenblatt DY, Kunnimalaiyaan M, & Chen H (2007) The HDAC inhibitor trichostatin A inhibits growth of small cell lung cancer cells. *J Surg Res* 142(2):219-226.
60. Komatsu N*, et al.* (2006) SAHA, a HDAC inhibitor, has profound anti-growth activity against non-small cell lung cancer cells. *Oncol Rep* 15(1):187-191.
61. Shakespear MR, Halili MA, Irvine KM, Fairlie DP, & Sweet MJ (2011) Histone deacetylases as regulators of inflammation and immunity. *Trends Immunol* 32(7):335-343.
62. Bray NL, Pimentel H, Melsted P, & Pachter L (2016) Near-optimal probabilistic RNA-seq quantification. *Nat Biotechnol* 34(5):525-527.
63. Soneson C, Love MI, & Robinson MD (2015) Differential analyses for RNA-seq: transcript-level estimates improve gene-level inferences. *F1000Res* 4:1521.
64. Risso D, Ngai J, Speed TP, & Dudoit S (2014) Normalization of RNA-seq data using factor analysis of control genes or samples. *Nat Biotechnol* 32(9):896-902.
65. Robinson MD, McCarthy DJ, & Smyth GK (2010) edgeR: a Bioconductor package for differential expression analysis of digital gene expression data. *Bioinformatics* 26(1):139-140.
66. Mi H*, et al.* (2017) PANTHER version 11: expanded annotation data from Gene Ontology and Reactome pathways, and data analysis tool enhancements. *Nucleic Acids Res* 45(D1):D183-D189.
67. Yu G, Wang LG, Han Y, & He QY (2012) clusterProfiler: an R package for comparing biological themes among gene clusters. *OMICS* 16(5):284-287.
68. Andrews NC & Faller DV (1991) A rapid micropreparation technique for extraction of DNA-binding proteins from limiting numbers of mammalian cells. *Nucleic Acids Res* 19(9):2499.

Figure Legends

Figure 1. Volatiles found in microbes can inhibit HDACs in vitro

(**A**) Antennal and whole mount brain staining of *Gr63a-Gal4* flies. Flies were exposed to diacetyl (headspace from 10^{-2} soln) or air for 2 to 5 days. Brains and antenna were dissected on the indicated days, fixed, and then stained for neuropil marker nc82 (red) and anti-GFP (green). (**B)** Mean of ab1C neurons expressing GFP after indicated days of odor exposure. d4on=2,3-butanedione. n=6, error bars=s.e.m. Schematic chemical structures of diacetyl, β-hydroxybutyrate and Sodium butyrate. **(C)** Dose-activity curves of class I HDACs: HDAC1, HDAC2, HDAC3, HDAC8 and class II HDAC6 treated with various concentrations of diacetyl. Percentage of HDAC activity is relative to the activity of each enzyme without diacetyl. IC50s are indicated in the chart areas. Error bars, S.E.M., n = 4-5. **(E)** Representative structures of odorants that inhibit HDACs, and **(F)** Average percentage inhibition of class I HDACs: HDAC1, HDAC3 and class II HDAC4, HDAC6 treated with 15mM of indicated volatiles. Error bar= S.D., each tested in duplicate.

Figure 2. Diacetyl increases level of histone acetylation in HEK293 cells

(A and B) Representative images from Western blots showing acetylation levels of H3K9 (left), H3K14 (middle) and H4K5 (right) in HEK293 cells after 2 hours **(A)** and 6 hours **(B)** of diacetyl exposure. PCNA (Proliferating cell nuclear antigen) is a 29 kDa nuclear protein used as a loading control for nuclear protein extracts. **(C)** Western blots showing acetylation levels of H3K9 in HEK293 cells treated with 100 μM diacetyl for 72, 96, and120 hours. PCNA is used for a loading control. **(D)** Bar graph showing the relative intensities of acetylated H3K9 in HEK293 cells treated with 100 μM diacetyl for 72 -120 hours. n = 4 samples, * $p < 0.05$, and **** $p < 0.0001$.

819 **Figure 3. Remote exposure to HDACi volatile alters gene expression in an invertebrate, and**
820 **vertebrate.**

821 (**A**) Schematic of odor exposure protocol for transcriptome analysis from the antennae. (**B**) Plot
822 highlighting up- and down-regulated genes in the diacetyl-exposed group. Red and blue dots
823 represent up-regulated genes (false discovery rate (FDR) < 0.05, $\log_2$ fold change (LFC) > 1) and
824 down-regulated genes (FDR < 0.05, LFC < 1), respectively. (**C**) Bar graphs denoting the protein
825 classification of the genes up- and down-regulated after odor exposure. **(D)** Schematic of diacetyl
826 exposure protocol for transcriptome analysis of mouse lung tissue. **(E)** Plot highlighting up- and
827 down-regulated genes in the diacetyl-exposed groups. Red and blue dots represent up-regulated
828 genes (FDR < 0.05, LFC > 1) and down-regulated genes (FDR < 0.05, LFC < 1), respectively in
829 lungs. **(F)** Table showing pairwise tests of significance of overlap between gene sets. P-values
830 from Fisher's exact test, colored with associated odds ratio (strength of association). **(G and H)**
831 Bar graphs denoting the protein classification of the genes up- and down-regulated in the lung after
832 0.1% **(G)** and 1% **(H)** of diacetyl exposure.

833 **Figure 4. Gene expression changes are partly reversible, and overlaps with known HDACi**
834 **drugs**

835 (**A**) Schematic of odor exposure and recovery protocol for transcriptome analysis from the
836 antennae. (**B**) Plot highlighting up- and down-regulated genes in the recovery from diacetyl
837 exposure group. Red and blue dots represent up-regulated genes (FDR < 0.05, LFC > 1) and down-
838 regulated genes (FDR < 0.05, LFC < 1), respectively. (**C**) Table showing pairwise tests of
839 significance of overlap between gene sets. P-values from Fisher's exact test, colored with
840 associated odds ratio (strength of association). (**D** and **E**) Plots showing enrichment of up- and

down-regulated genes in sodium butyrate- (**D**) and valproic acid-treated (**E**) groups. Red and blue dots represent up-regulated genes (FDR < 0.05, LFC > 1) and down-regulated genes (FDR < 0.05, LFC < 1), respectively. (**F**) *Left:* Venn diagrams showing the overlaps of up-regulated genes among diacetyl-, sodium butyrate- and valproic acid-treated groups. *Right:* Table showing pairwise tests of significance of overlap between gene sets. P-values from Fisher's exact test. (**G and H)** GO-enrichment analysis of the common Up-regulated and down-regulated genes across all 3 treatments in (**F**)**.**

Figure 5. Exposure to diacetyl vapor alters gene expression in the mouse brain

(A) Schematic of diacetyl exposure protocol for transcriptome analysis of mouse brain tissues. **(B and C)** Plot showing up- and down-regulated genes in the diacetyl-exposed groups. Red and blue dots represent up-regulated genes (FDR < 0.05, LFC > 1) and down-regulated genes (FDR < 0.05, LFC < 1), respectively in the brain. **(D)** *Left:* Table showing pairwise tests of significance of overlap between gene sets. P-values from Fisher's exact test. *Right:* Venn diagrams showing the overlaps of DEGs between lung and brain groups. **(E)** Bar graphs denoting the protein classification of the brain genes up- and down-regulated after 1% diacetyl exposure. **(F)** Mean fold change of select neuroblastoma related genes in the brain of mice exposed to diacetyl vapors. **(G)** Cell counts of indicated cancer cell lines in tissue culture treated with solvent control or indicated concentration of diacetyl. N=3-6, p<0.001.

Figure 6. Odor exposure slows Huntington's neurodegeneration model in fly eye

862 **(A)** Schematic diagram showing temperature of experimental condition and timing of the eye
863 examination in pGMR-HTTQ120 flies. **(B)** Bar graph showing mean number of rhabdomeres in
864 each ommatidium in solvent paraffin oil (PO, blue) and diacetyl-exposed (red) pGMR-HTTQ120
865 flies at 1, 5, and 10 days after eclosion (AE). n = 600 ommatidia from 15 flies, **** $p < 0.0001$.
866 **(C)** A representative image of ommatidia of pGMR-HTTQ120 flies at 1 day AE. **(D and E)**
867 Representative images of ommatidia of pGMR-HTTQ120 flies exposed to paraffin oil (PO) or
868 diaceyl at 5 **(D)** and 10 **(E)** days AE. **(F and G)** Histogram showing the percent of the ommatidium
869 with a given number of rhabdomeres indicated on the x axis at 5 **(F)** and 10 **(G)** days AE.

870

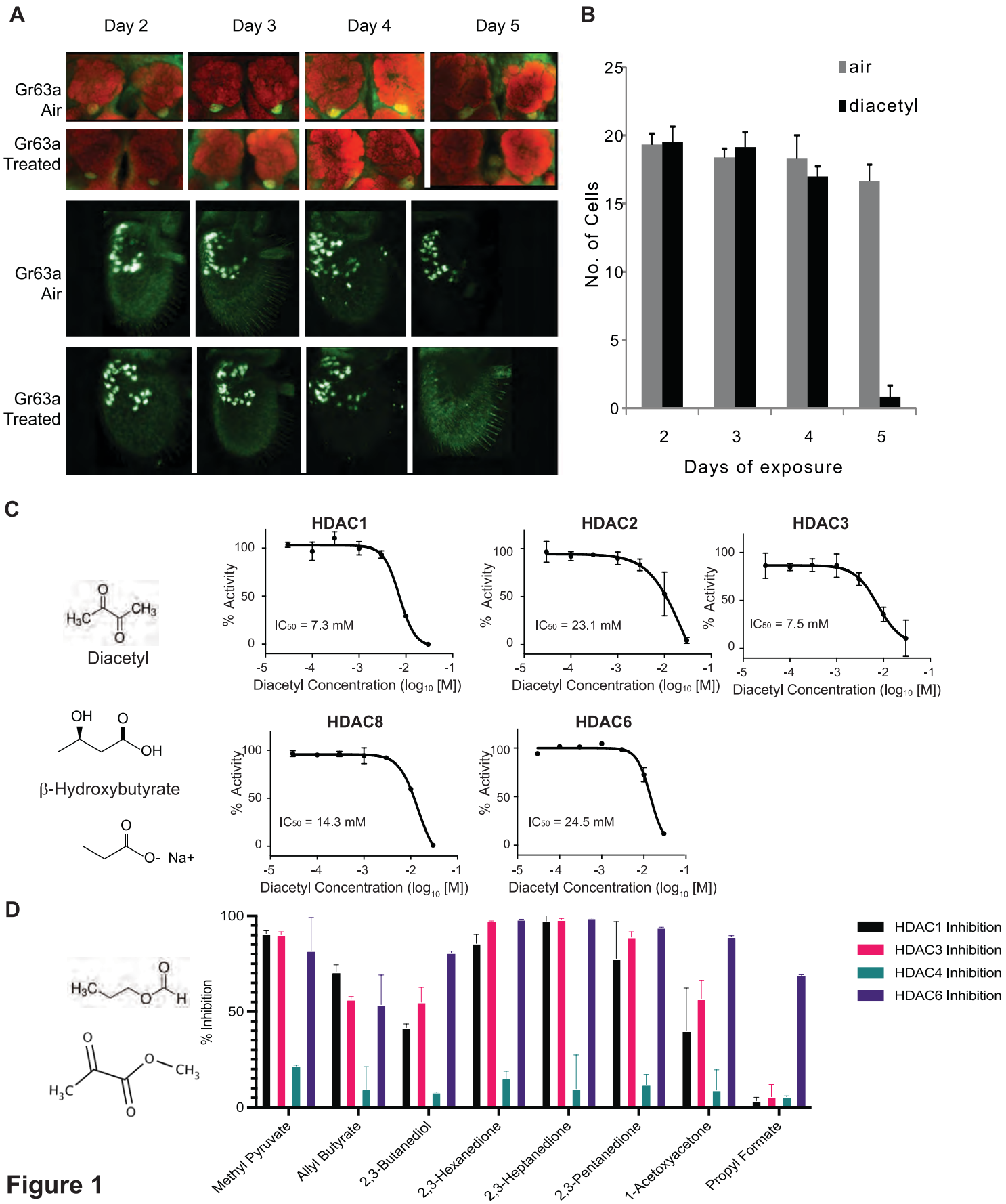
A
Day 2
Day 3
Day 4
Day 5
Gr63a Air
Gr63a Treated
Gr63a Air
Gr63a Treated
B
air
diacetyl
No. of Cells
Days of exposure
C
Diacetyl
β-Hydroxybutyrate
HDAC1
HDAC2
HDAC3
HDAC8
HDAC6
% Activity
IC50 = 7.3 mM
IC50 = 23.1 mM
IC50 = 7.5 mM
IC50 = 14.3 mM
IC50 = 24.5 mM
Diacetyl Concentration (log10 [M])
D
% Inhibition
HDAC1 Inhibition
HDAC3 Inhibition
HDAC4 Inhibition
HDAC6 Inhibition
Methyl Pyruvate
Allyl Butyrate
2,3-Butanediol
2,3-Hexanedione
2,3-Heptanedione
2,3-Pentanedione
1-Acetoxyacetone
Propyl Formate

Figure 1

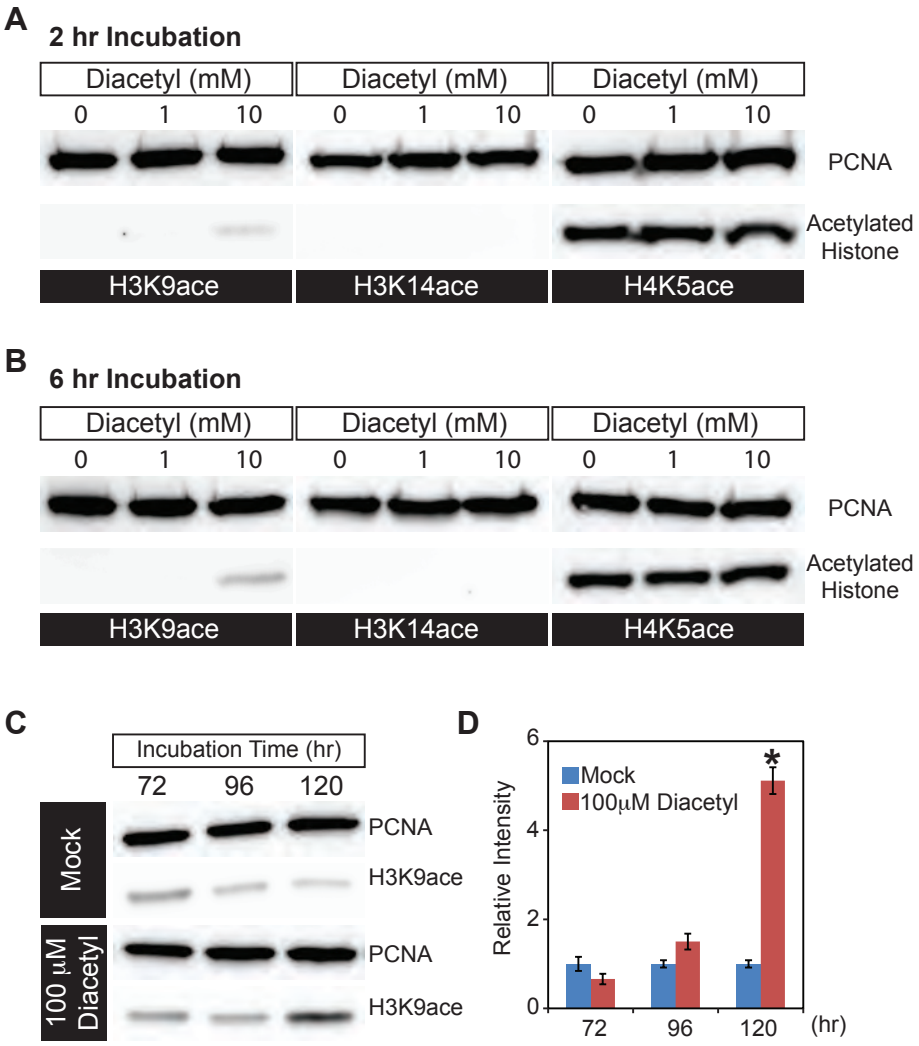
A
2 hr Incubation
Diacetyl (mM)
0 1 10
PCNA
Acetylated Histone
H3K9ace
H3K14ace
H4K5ace
B
6 hr Incubation
C
Incubation Time (hr)
72 96 120
Mock
100 μM Diacetyl
D
Mock
100μM Diacetyl
Relative Intensity
(hr)

Figure 2

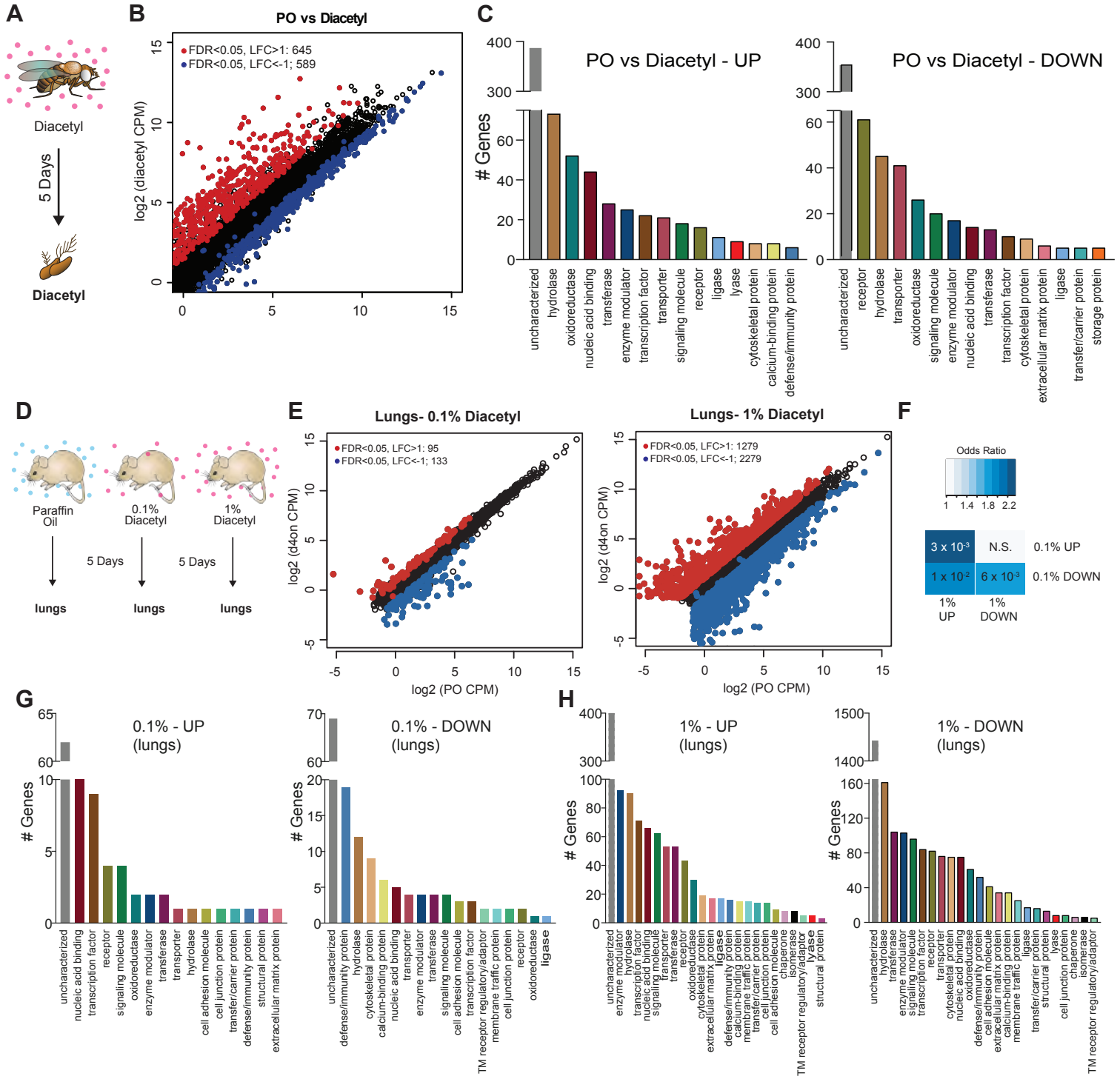
A
Diacetyl
5 Days
Diacetyl
B
PO vs Diacetyl
FDR<0.05, LFC>1: 645
FDR<0.05, LFC<-1; 589
log2 (diacetyl CPM)
C
PO vs Diacetyl - UP
PO vs Diacetyl - DOWN
Genes
uncharacterized
hydrolase
oxidoreductase
nucleic acid binding
transferase
enzyme modulator
transcription factor
transporter
signaling molecule
receptor
ligase
lyase
cytoskeletal protein
calcium-binding protein
defense/immunity protein
extracellular matrix protein
storage protein
transfer/carrier protein
D
Paraffin Oil
0.1% Diacetyl
1% Diacetyl
5 Days
5 Days
lungs
lungs
lungs
E
Lungs- 0.1% Diacetyl
FDR<0.05, LFC>1: 95
FDR<0.05, LFC<-1; 133
Lungs- 1% Diacetyl
FDR<0.05, LFC>1: 1279
FDR<0.05, LFC<-1; 2279
log2 (d4on CPM)
log2 (PO CPM)
F
Odds Ratio
1 1.4 1.8 2.2
3 x 10-3
N.S.
0.1% UP
1 x 10-2
6 x 10-3
0.1% DOWN
1% UP
1% DOWN
G
0.1% - UP (lungs)
0.1% - DOWN (lungs)
H
1% - UP (lungs)
1% - DOWN (lungs)
Genes

Figure 3

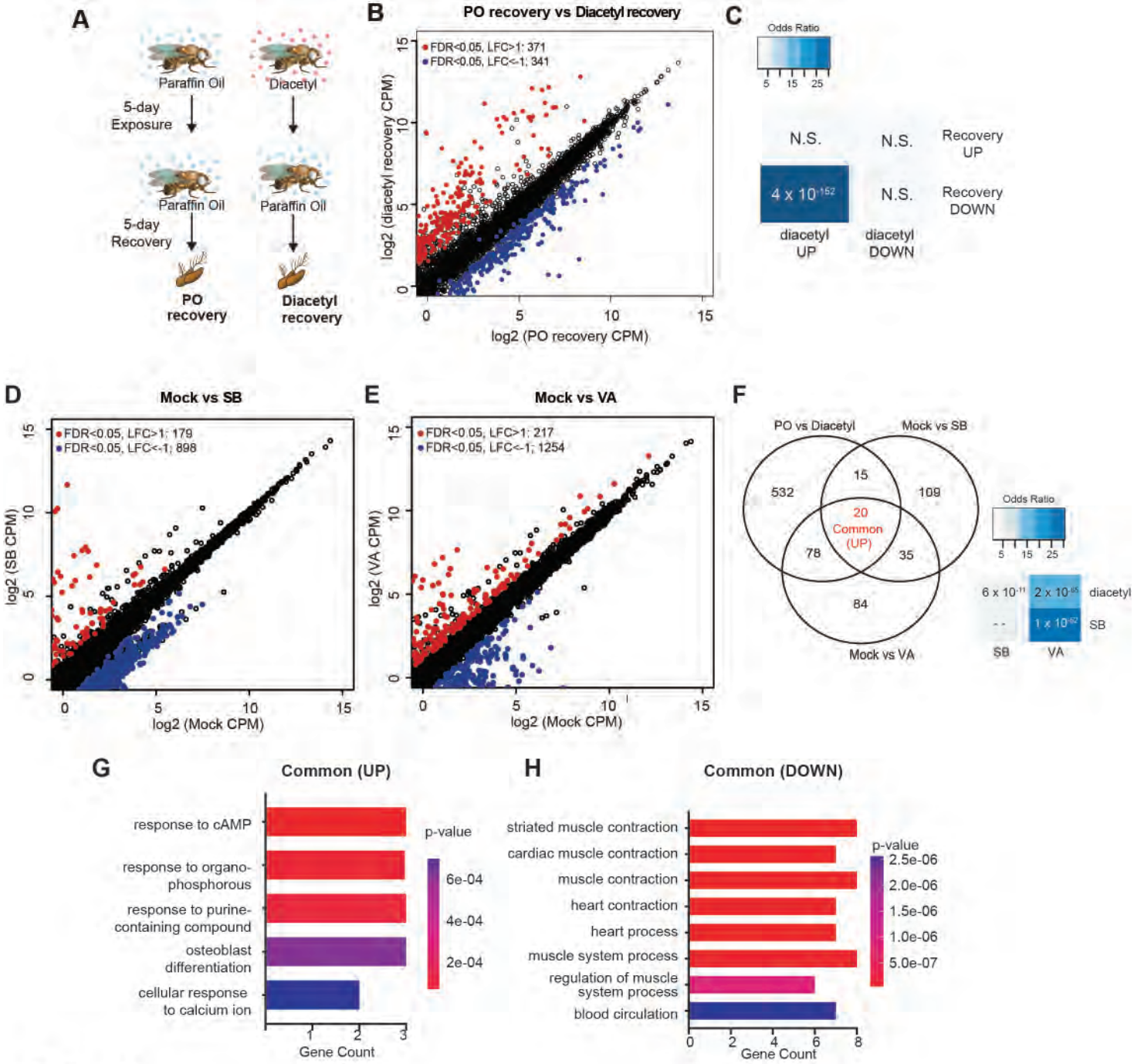
A
Paraffin Oil
Diacetyl
5-day Exposure
Paraffin Oil
Paraffin Oil
5-day Recovery
PO recovery
Diacetyl recovery
B
PO recovery vs Diacetyl recovery
FDR<0.05, LFC>1: 371
FDR<0.05, LFC<-1: 341
log2 (diacetyl recovery CPM)
log2 (PO recovery CPM)
C
Odds Ratio
5 15 25
N.S.
N.S.
Recovery UP
4 x 10-152
N.S.
Recovery DOWN
diacetyl UP
diacetyl DOWN
D
Mock vs SB
FDR<0.05, LFC>1: 179
FDR<0.05, LFC<-1: 898
log2 (SB CPM)
log2 (Mock CPM)
E
Mock vs VA
FDR<0.05, LFC>1: 217
FDR<0.05, LFC<-1: 1254
log2 (VA CPM)
log2 (Mock CPM)
F
PO vs Diacetyl
Mock vs SB
Mock vs VA
532
15
109
20 Common (UP)
78
35
84
Odds Ratio
5 15 25
6 x 10-11
2 x 10-85
diacetyl
- -
1 x 10-52
SB
SB
VA
G
Common (UP)
response to cAMP
response to organo-phosphorous
response to purine-containing compound
osteoblast differentiation
cellular response to calcium ion
p-value
6e-04
4e-04
2e-04
Gene Count
H
Common (DOWN)
striated muscle contraction
cardiac muscle contraction
muscle contraction
heart contraction
heart process
muscle system process
regulation of muscle system process
blood circulation
p-value
2.5e-06
2.0e-06
1.5e-06
1.0e-06
5.0e-07
Gene Count

Figure 4

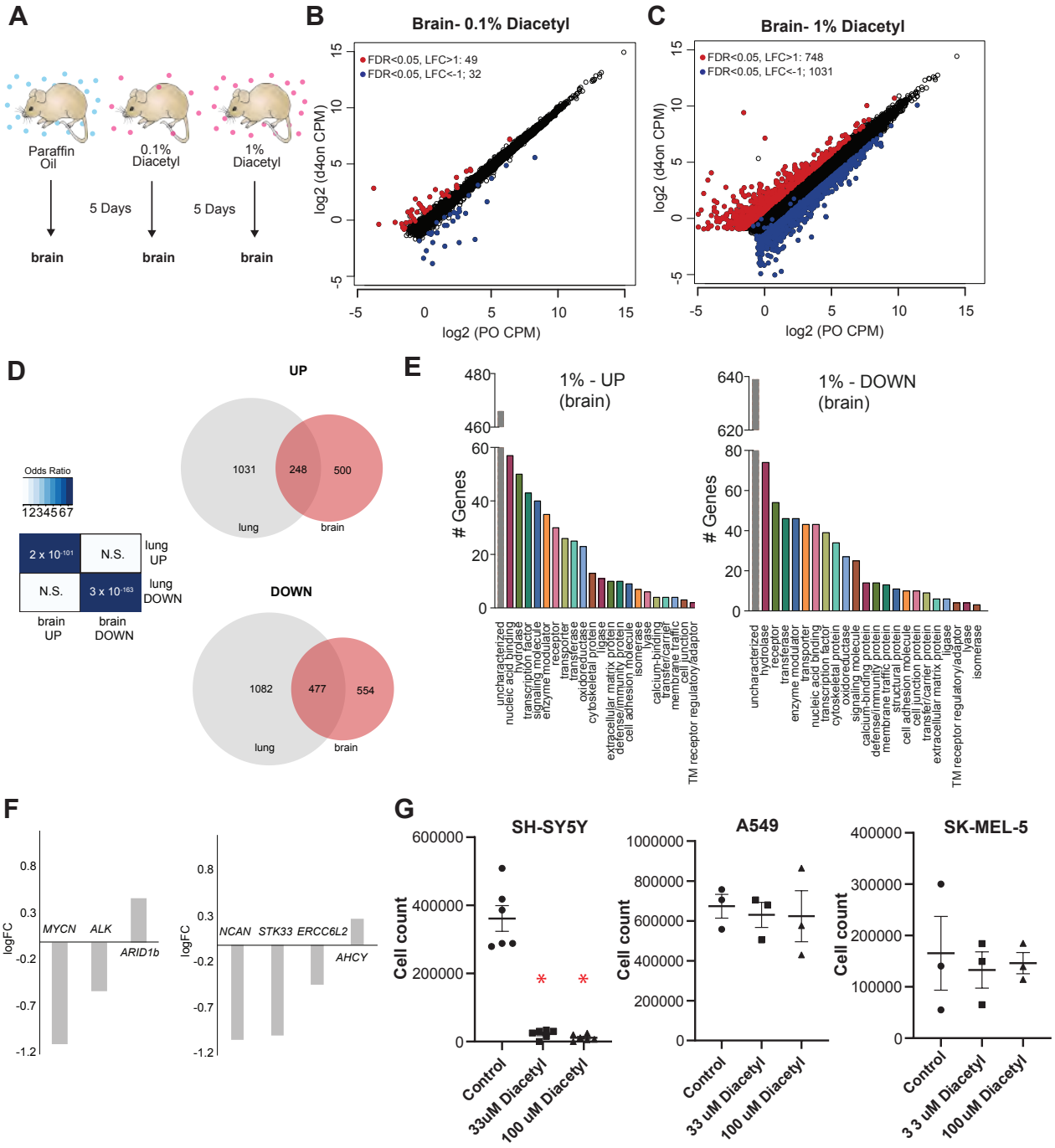
A
Paraffin Oil
0.1% Diacetyl
1% Diacetyl
5 Days
5 Days
brain
brain
brain
B
Brain- 0.1% Diacetyl
FDR<0.05, LFC>1: 49
FDR<0.05, LFC<-1; 32
log2 (d4on CPM)
log2 (PO CPM)
C
Brain- 1% Diacetyl
FDR<0.05, LFC>1: 748
FDR<0.05, LFC<-1; 1031
log2 (d4on CPM)
log2 (PO CPM)
D
Odds Ratio
1234567
2 x 10-101
N.S.
N.S.
3 x 10-163
lung UP
lung DOWN
brain UP
brain DOWN
UP
1031
248
500
lung
brain
DOWN
1082
477
554
lung
brain
E
1% - UP (brain)
1% - DOWN (brain)
Genes
uncharacterized
hydrolase
receptor
transferase
enzyme modulator
transporter
nucleic acid binding
transcription factor
cytoskeletal protein
oxidoreductase
signaling molecule
calcium-binding protein
defense/immunity protein
membrane traffic protein
structural protein
cell adhesion molecule
cell junction protein
transfer/carrier protein
extracellular matrix protein
ligase
TM receptor regulatory/adaptor
lyase
isomerase
F
logFC
MYCN
ALK
ARID1b
NCAN
STK33
ERCC6L2
AHCY
G
SH-SY5Y
A549
SK-MEL-5
Cell count
Control
33uM Diacetyl
100 uM Diacetyl
33 uM Diacetyl
3 3 uM Diacetyl

Figure 5

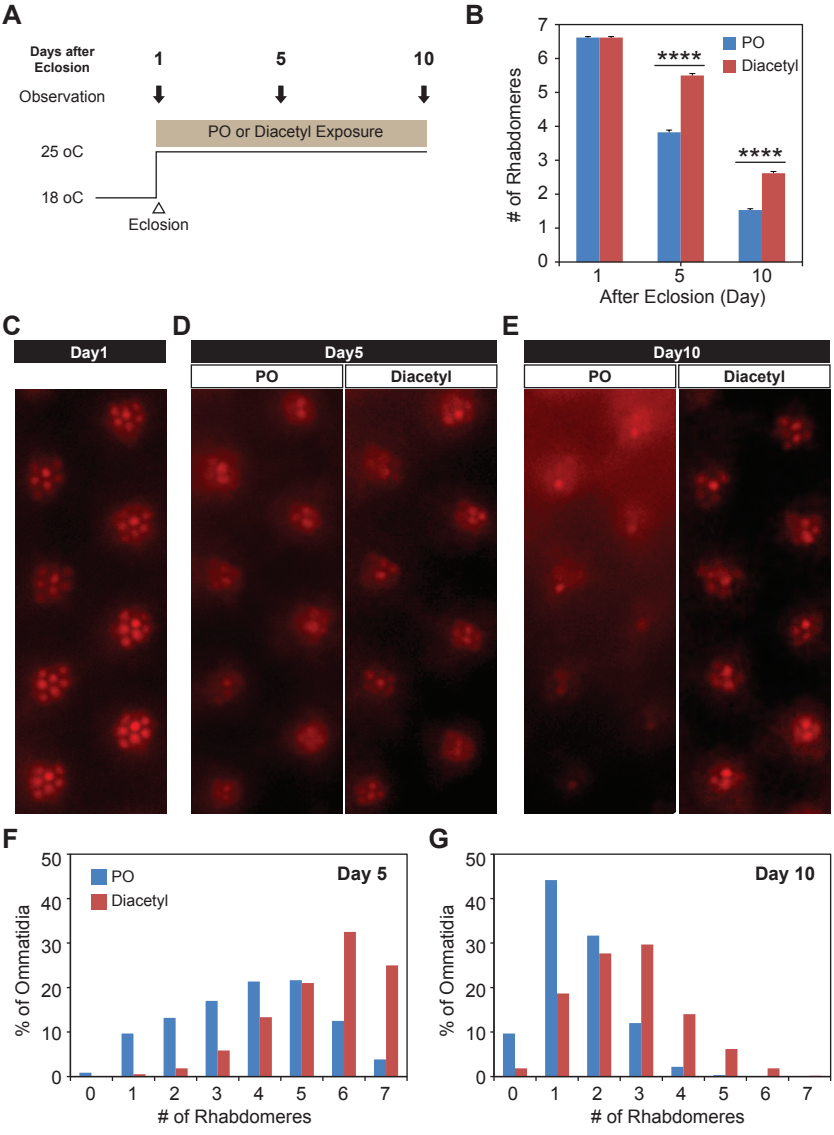
A
Days after Eclosion
1
5
10
Observation
PO or Diacetyl Exposure
25 oC
18 oC
Eclosion
B
PO
Diacetyl
****
****
# of Rhabdomeres
After Eclosion (Day)
C
Day1
D
Day5
PO
Diacetyl
E
Day10
PO
Diacetyl
F
PO
Diacetyl
Day 5
% of Ommatidia
# of Rhabdomeres
G
Day 10
% of Ommatidia
# of Rhabdomeres

Figure 6